A Volcano Rekindled: The Renewed Eruption of Mount St. Helens, 2004–2006
Edited by David R. Sherrod, William E. Scott, and Peter H. Stauffer
U.S. Geological Survey Professional Paper 1750, 2008

Chapter 14

Constraints and Conundrums Resulting from Ground-Deformation Measurements Made During the 2004–2005 Dome-Building Eruption of Mount St. Helens, Washington

By Daniel Dzurisin[1], Michael Lisowski[1], Michael P. Poland[2], David R. Sherrod[1], and Richard G. LaHusen[1]

Abstract

A prolonged period of dome growth at Mount St. Helens starting in September–October 2004 provides an opportunity to study how the volcano deforms before, during, and after an eruption by using modern instruments and techniques, such as global positioning system (GPS) receivers and interferometric synthetic aperture radar (InSAR), together with more traditional ones, including tiltmeters, triangulation, photogrammetry, and time-lapse photography. No precursory ground deformation was detected by campaign GPS measurements made in 2000 and 2003, nor by a continuous GPS station (JRO1) operating ~9 km to the north-northwest of the vent area since May 1997. However, JRO1 abruptly began moving downward and southward, toward a source centered about 8 km beneath the volcano, concurrently with the start of a shallow earthquake swarm on September 23, 2004. The JRO1 velocity slowed from ~0.5 millimeters per day (mm/d) in late September–early October 2004 until spring 2005. Thereafter, it was essentially constant at ~0.04 mm/d through December 2005. In similar fashion, the growth rate of the welt on the south crater floor slowed from 8.9 m^3/s during October 4–11 to 6.4 m^3/s during October 11–13, 2004; this trend continued after emergence of the first lava spine on October 11. The volumetric extrusion rate decreased from 5.9 m^3/s during October 13–November 4, 2004, to 2.5 m^3/s during December 11, 2004–January 3, 2005, and for the remainder of 2005, it was in the range 2.0–0.7 m^3/s. Fifteen continuous GPS stations, installed soon after the eruption began, showed radially inward and downward ground motions through December 2005. Likewise, InSAR observations spanning the first year of the eruption indicate broad subsidence centered near the vent. Model-derived estimates of source-volume decrease from September 23, 2004, to October 31, 2006, are $16–24\times10^6$ m^3, substantially less than the volume erupted during the same period (87×10^6 m^3 through October 21, 2006). The discrepancy can be explained by a combination of magma expansion and recharge in the source region.

Lack of precursory deformation at JRO1 suggests that the conduit is poorly coupled to the rest of the edifice, so the rising magma column was able to push ahead older conduit material rather than intruding it. Constraints on conduit length and radius require that reservoir magma (as opposed to conduit-filling magma) reached the surface early during the eruption, probably soon after CO_2 emission rates peaked in early October 2004. If rapid emergence of spine 3 (the first whaleback-shaped extrusion) in late October 2004 marked the arrival of reservoir magma, then the volume of conduit material flushed from the system was about 20×10^6 m^3—the volume of surface deformation plus spines on November 4, 2004. The corresponding radius for a cylinder extending from the surface to depth d = 5 km is 35.7 m, or 28.2 m for d = 8 km. The average ascent rate through the conduit, assuming reservoir magma began its rise on September 23, 2004, was 120 m/d for d = 5 km, or 190 m/d for d = 8 km. Observed lineal extrusion rates were 2–10 m/d, so the conduit must widen considerably near the surface. Equating magma flux through the conduit to that at the surface, we obtain a vent radius of 125 m and an extrusion rate of 5.7 m^3/s—both values representative of the early part of the eruption.

Lack of precursory inflation suggests that the volcano was poised to erupt magma already stored in a crustal reservoir when JRO1 was installed in 1997. Trilateration and campaign GPS data indicate surface dilatation, presumably caused by reservoir expansion between 1982 and 1991, but no measurable deformation between 1991 and 2003. We conclude that all three of the traditionally reliable eruption

[1] U.S. Geological Survey, 1300 SE Cardinal Court, Vancouver, WA 98683

[2] U.S. Geological Survey, PO Box 51, Hawaii National Park, HI 96718

precursors (seismicity, ground deformation, and volcanic gas emission) failed to provide warning that an eruption was imminent until a few days before a visible welt appeared at the surface—a situation reminiscent of the 1980 north-flank bulge at Mount St. Helens.

Introduction

The deformational behavior of active basaltic shield volcanoes and large silicic magmatic systems (restless calderas) can be characterized in a general way by, respectively, (1) repeated inflation-deflation cycles in response to changes in crustal magma storage (for example, Kīlauea, Hawai‘i, U.S.A., Dvorak and Okamura, 1987; Krafla, Iceland, Tryggvason, 1994), and (2) episodes of more gradual surface uplift or subsidence (bradyseisms) caused by magmatic inflation-deflation or hydrothermal system pressurization-depressurization (for example, Long Valley Caldera, Calif., U.S.A., Hill and others, 1985; Yellowstone caldera[3], Wyo., U.S.A., Dzurisin and others, 1999; Wicks and others, 2006; Phlegraean Fields caldera, Italy, Caputo, 1979). Deformation of stratovolcanoes of intermediate composition (andesite–dacite) is more varied and therefore more difficult to understand. Nonetheless, volcanoes of this type are numerous along the Pacific margin and, on short to intermediate time scales, they pose a greater threat to human populations than do basaltic shields or large silicic systems.

The reawakening of Mount St. Helens in 1980 following 123 years of quiescence provided a modern opportunity to study pre-, syn-, and post-eruptive deformation at an accessible and relatively well-studied stratovolcano. However, little was learned about any deep-seated deformation (source depth more than ~2 km) that might have occurred before the eruption because magma rose to shallow depth—as evidenced by the appearance of a bulge on the volcano's north flank by early April 1980 (fig. 1*A*)—before or soon after March 20, 1980, when a swarm of earthquakes caught volcanologists' attention and spurred the start of intensive monitoring (Lipman and others, 1981).

Renewed dome growth at Mount St. Helens starting in September–October 2004 (fig. 1*B*) provides a second opportunity to study how this volcano deforms before, during, and after an eruption—this time by using modern geodetic instruments and techniques, such as Global Positioning System (GPS) receivers (Lisowski and others, this volume, chap. 15; LaHusen and others, this volume, chap. 16) and interferometric synthetic aperture radar (InSAR, Poland and Lu, this volume, chap. 18), together with more traditional instruments and techniques, including tiltmeters, triangulation, photogrammetry, and time-lapse photography (Poland and others, this volume, chap. 11; Major and others, this volume, chap. 12). Deformation data from the first 15 months of the eruption (October 2004–December 2005) help to constrain (1) the depth and geometry of the magma plumbing system and (2) the time history of magma outflow and possible recharge to a crustal magma reservoir (Lisowski and others, this volume, chap. 15; Mastin and others, this volume, chap. 22). The 2004–5 deformation data, especially when considered together with other datasets, also raise several new questions.

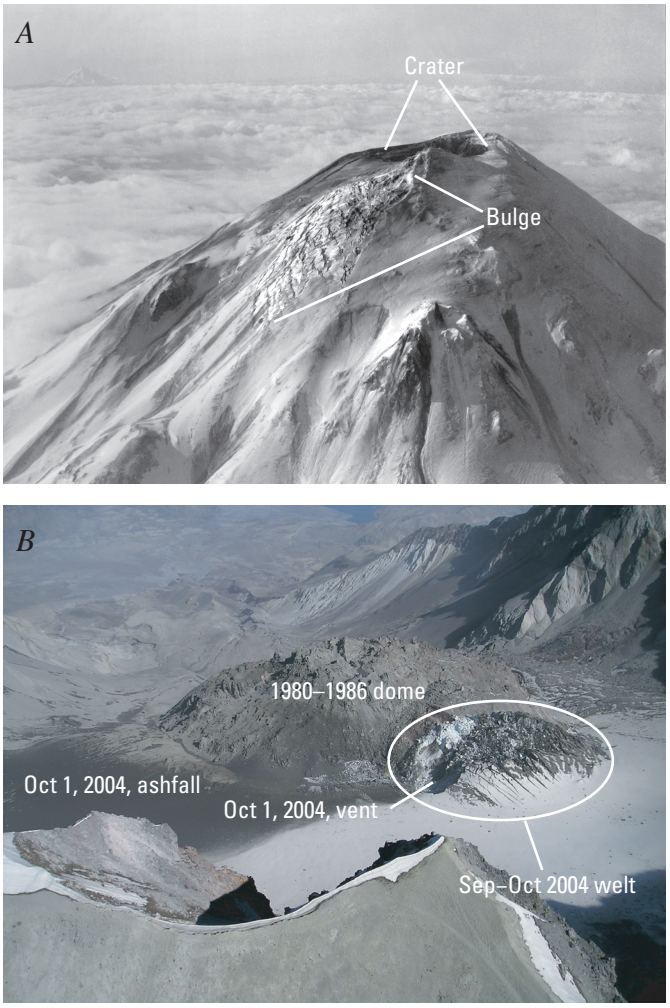

Figure 1. Examples of precursory surface deformation before eruptions at Mount St. Helens, Washington. *A*, Upper north flank on April 7, 1980. Series of phreatic eruptions that began on March 27, 1980, deposited ash and formed summit crater, which had grown to about 500 m west-east and 300 m north-south. Intensely cracked area below and north of crater shows distension of north flank. USGS photograph by R.B. Waitt. *B*, Crater floor as seen from above southwest crater rim on October 3, 2004. Vent for October 1 ash is visible at the west base of the welt of uplifted crater floor and glacial ice first recognized as deforming on September 27, 2004. USGS photograph by S. Konfal.

[3] Capitalization of "Caldera" or "Volcano" indicates adoption of the word as part of the formal geographic name by the host country, as listed in the Geographic Names Information System, a database maintained by the U.S. Board on Geographic Names. Noncapitalized "caldera" or "volcano" is applied informally—eds.

This paper draws freely on datasets and analyses presented elsewhere in this volume. Its main objectives are (1) to present an integrated overview of ground deformation observations, measurements, and results through December 2005 and (2) to explore some implications of these results, together with those from other disciplines, for the mechanism of the eruption and its future course.

Geodetic Techniques Used to Study the Eruption

This section summarizes the techniques used, successfully or unsuccessfully, to measure ground deformation during the 2004–5 eruption. The reader is referred to other papers in this volume for more thorough treatments of some of the techniques, results, and interpretations.

Regional Trilateration and Campaign-Style GPS Measurements

The Helens high-precision trilateration network was established in 1982 to track regional strain accumulation following the 1980 eruption at Mount St. Helens. Line lengths were measured with a Geodolite in 1982 and 1991 and with GPS in 2000. Lisowski and others (this volume, chap. 15) report that line lengths consistently increased by 1–3 cm between 1982 and 1991 but did not change significantly from 1991 to 2000. The line-length increases correspond to areal dilatation at a rate of 144±39 nanostrain/yr, which is an order of magnitude greater and distinctly different than the background tectonic strain. Lisowski and others (this volume, chap. 15) discount possible systematic error in the Geodolite surveys as the sole reason for the observed dilatation and invoke "… some other phenomenon, like recharge of the magma reservoir…" to account for the observations.

During summer 2000, the USGS Cascades Volcano Observatory (CVO) installed and made initial GPS observations at more than 40 benchmarks on and around Mount St. Helens (herein referred to as the large-aperture GPS network). The network is concentrated within 10 km of the volcano, but it extends more than 30 km and covers an area of more than 7,400 km^2 (fig. 2; Dzurisin, 2003). The first repeat survey was made in summer 2003. With effects of rigid-block rotation and regional strain removed, no significant strain was detected, with one exception: a station (DMSH) on the 1980–86 lava dome (fig. 2) moved down and east-northeastward, toward the center of the dome, at average rates of 9.0 cm/yr and 2.9 cm/yr, respectively (Lisowski and others, this volume, chap. 15).

The motion of DMSH is consistent with that seen at several nearby stations on the 1980–86 dome, which were observed each summer from 2000 to 2004 to provide geodetic control for vertical air photos and digital elevation models (Schilling and others, this volume, chap. 8). These stations generally moved down and toward the center of the dome at rates of a few centimeters per year, while stations on the crater floor moved very little (Lisowski and others, this volume, chap. 15). The motion of the stations is attributed to cooling and compaction of the uppermost conduit and dome. The latter consists mainly of stubby, highly deformed, dacite lava flows (lobes) and bouldery talus (Swanson and others, 1987). There is no evidence from the August 2004 control-point survey data of any change in trend that could be associated with the start of the current eruption.

The regional trilateration and campaign GPS data indicate that most of the surface deformation prior to the 2004–5 eruption took place in the decade following the 1980 eruption, and that little or no surface deformation occurred between 1991 and 2003. This is consistent with data from continuous GPS (CGPS) station JRO1, 8 km north-northwest of the volcano, which recorded no volcano-centric deformation from May 1997 to the beginning of seismic unrest on September 23, 2004 (see below). However, there is seismic evidence for pressurization of the magma reservoir and upward fluid intrusion starting in late 1987 and continuing at least until November 2001 (Moran, 1994; Moran and others, this volume, chap. 2). This apparent contradiction and other questions are addressed in the later Discussion section.

Continuous GPS (CGPS)

Johnston Ridge Observatory (JRO1)

Included in the large-aperture GPS network are 17 CGPS stations on or close to the volcano. The first station, JRO1, was installed in May 1997 at the Mount St. Helens National Volcanic Monument's Johnston Ridge Observatory. Lisowski and others (this volume, chap. 15) conclude that, within uncertainties, (1) the velocity of JRO1 was constant from May 1997 through mid-September 2004, and (2) JRO1 abruptly started moving south-southeast and down, toward a source beneath Mount St. Helens, on or about September 23, 2004. The anomalous motion was essentially concurrent (±1 day) with the start of a shallow earthquake swarm beneath the crater floor (Moran and others, this volume, chap. 2). Seismicity was accompanied by the growth of a large welt (fig. 1*B*), which was first visible in photographs taken on September 26. The first of several lava spines emerged from the welt on October 11, and extrusion of a dacite dome continued through the end of 2005 (Dzurisin and others, 2005; Vallance and others, this volume, chap. 9).

Fresh crevasses in glacier ice on the south crater floor, indicating intense deformation of the area that was to become the welt, were first recognized a few days after the start of shallow seismicity and anomalous motion at JRO1. New crevassing and uplift were confirmed by direct observation on September 29, 2004. In hindsight, they were recognized in photographs taken on September 26 by J.S. Pallister during

a fixed-wing observation flight. Helicopter pilot Jeff Linscott (JL Aviation, Inc.) first noticed new cracks in the ice on September 28 while flying with members of the news media. He pointed out the cracks to us (D. Dzurisin and M.P. Poland) the next day, September 29. A photograph taken by a hiker from the south crater rim on September 25 shows no obvious disturbance in the area that became the welt; thus, the first surface cracks probably formed 2–3 days after the start of a shallow earthquake swarm at about 0200 PDT (0900 UTC) on September 23 and within 1 day of an uptick in seismicity on September 25 that culminated with the onset of the eruption.

On August 27, 2004, Linscott landed in the southern part of the crater with USGS–CVO staff; fresh cracks in glacier ice at their customary landing site forced them to use an alternate site nearby. Any significance of those cracks in terms of the impending eruption is undocumented. At the time, the cracks were attributed to summer snowmelt revealing crevasses in the advancing glacier. Similar features had been seen before and were visible at the time on the west arm of the glacier. Any relation to the recognized onset of volcanic unrest nearly a month later is speculative and not supported by the hiker's photograph taken on September 25.

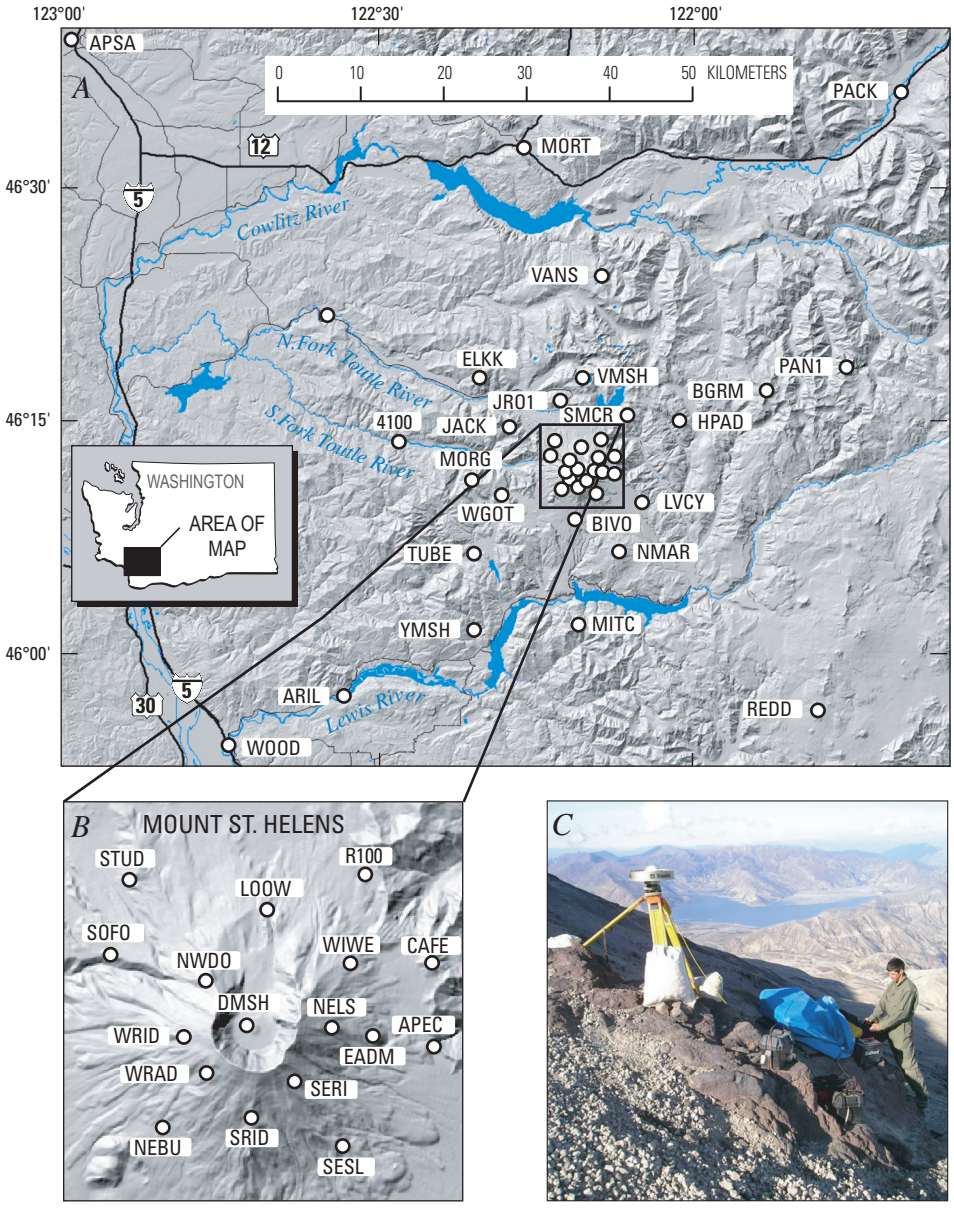

Figure 2. Large-aperture GPS network at Mount St. Helens, Washington. *A*, Location map showing 40 benchmarks observed during summers of 2000 and 2003. Base from shaded relief version of USGS digital elevation model. *B*, Benchmarks on or near the volcano. *C*, GPS receiver deployed at NELS (Nelson Ridge) on upper east flank of Mount St. Helens in October 2004.

Following a period of rapid motion toward a source beneath the volcano at a peak rate of ~0.5 mm/d in late September–early October 2004 (while the growth rate of the welt was as high as 8.9 m^3/s), the movement of JRO1 gradually slowed through December 2004. Meanwhile, the extrusion rate slowed from 5.9 m^3/s (October 13–November 4) to 2.5 m^3/s (December 11, 2004–January 3, 2005; Schilling and others, this volume, chap. 8). During May–December 2005, the velocity of JRO1 was essentially constant at ~0.04 mm/d toward the volcano. During the same interval, the rate of lava extrusion declined from 1.3 m^3/s (April 19–June 15) to 0.7 m^3/s (October 24–December 15), with somewhat higher rates during July 14–August 10 (2.0 m^3/s) and August 10–September 20 (1.6 m^3/s; Schilling and others, this volume, chap. 8).

Mount St. Helens CGPS Cluster

In response to the current eruption, CVO and the EarthScope Plate Boundary Observatory (PBO) installed 13 additional CGPS stations during October–November 2004. Most of the new stations are on the volcano, mounted 3–4 m high on steel tripods that served as EDM stations during the 1980s (fig. 3). Data from all 14 CGPS stations at Mount St. Helens are downloaded automatically to CVO and to the UNAVCO Boulder Facility Archive. The data are processed daily at the USGS Menlo Park facility to produce a 24-hour solution. Five additional stations, mounted on smaller tripods and without telemetry links, have operated intermittently since November 2004. Data from those stations are downloaded manually.

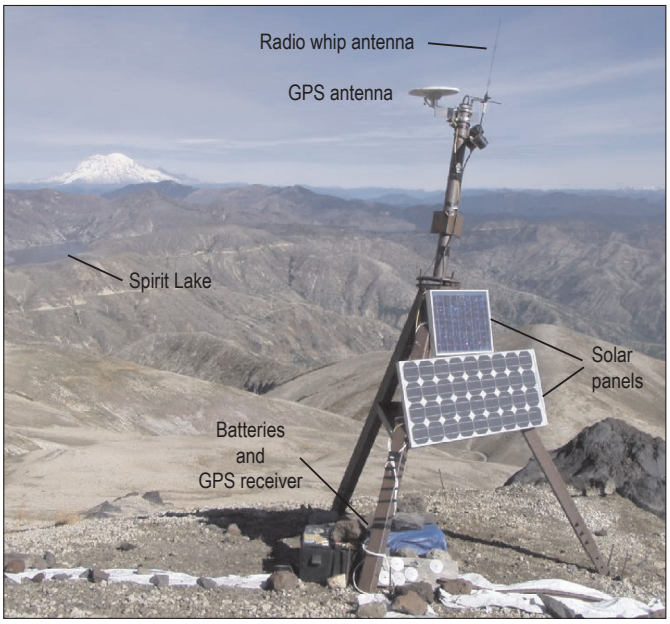

Figure 3. CGPS station WIWE (Windy West) on lower northeast flank of Mount St. Helens, Washington (fig. 2). Station is typical of several installed by CVO. View is to north-northeast. Mount Rainier is visible 77 km in distance.

Time-series plots of CGPS data show that the rate of motion toward the volcano peaked in late September or early October 2004, while the welt was growing rapidly but before the first lava emerged on October 11, 2004 (see figs. 10–13 in Lisowski and others, this volume, chap. 15). Both the far-field (beyond the crater floor) deformation rate and the extrusion rate declined progressively from mid-October through at least December 2004. Perhaps as early as January 2005, and surely by May 2005, the deformation rate and extrusion rate stabilized; both rates were relatively steady through December 2005.

Single-Frequency (L1-Only) GPS "Spiders"

It was clear from the early days of the eruption that extreme deformation of the south crater floor and glacier must attenuate rapidly with distance, because the 1980–86 dome and crater floor to the north remained essentially undisturbed, while the welt, just a few hundred meters to the south, grew to 500 m west-east, 600 m north-south, and 110–120 m high by October 11, 2004. LaHusen and others (this volume, chap. 16) report that a single-frequency CGPS station at SEP, on the 1980–86 dome less than 500 m north of the 2004–5 vent, moved anomalously about 20 cm north, 8 cm west, and 12 cm up during the 9-month period ending on September 27, 2004. This displacement was much less than we expected, given the large size and proximity of the welt. Likewise, all 13 of the CGPS stations that were installed on the volcano's flanks during October–November 2004 moved less than 2 cm during the ensuing 15 months. Therefore, it was necessary to install deformation sensors within a few hundred meters of the vent to monitor the course of the eruption. Conventional CGPS installations were not a reasonable option, because instrumentation in proximal areas had an expected lifetime of only days or weeks during the first few months of the eruption. Instead, we deployed and, in some cases, retrieved and redeployed a series of single-frequency (L1-only) CGPS stations aboard "spiders"—self-contained sensor platforms slung from a helicopter to otherwise inaccessible or hazardous sites (LaHusen and others, this volume, chap. 16). Here we summarize results of three GPS spider deployments to the growing dome, which provided reliable measurements of lineal extrusion rates for spines 3 and 4. See LaHusen and others (this volume, chap. 16) for discussion of additional deployments to the 2004–5 dome, 1980–86 dome, and Crater Glacier.

On November 20, 2004, GPS spider ELEA was set down astride spine 3, which was advancing south-southeastward across the crater floor. During the ensuing six days, before the instrument was destroyed in a rockfall, ELEA traveled 67 m southeast and 8 m up at an average rate of ~10 m/d and an average slope of 5.6° (LaHusen and others, this volume, chap. 16). The GPS spider CDAN was destroyed by a small explosive event starting at 0318 PST on January 16, 2005 (Scott and others, this volume, chap. 1), about 36 hours after it was deployed to spine 4. In the preceding 24 hours, CDAN moved 6.5 m south, 2.2 m east, and 4.7 m up, corresponding

to an average velocity of 8.3 m/d at an average slope of 34.5°. The GPS spider AHAD was deployed to spine 4 on February 8, 2005. By the time it was retrieved on February 16, AHAD had moved 29 m south, 17 m east, and 9 m up, for an average velocity of 6.2 m/day at an average slope of 15.5° (LaHusen and others, this volume, chap. 16).

Velocities measured by ELEA, CDAN, and AHAD are not directly comparable for two reasons: (1) spines 3 and 4 differed in morphology (4 was, for the most part, steeper than 3), and (2) the three spiders occupied different positions with respect to the vent. Nonetheless, slowing of the extrusion velocity between late November 2004 and mid-February 2005, as indicated by the GPS spiders, is consistent with analysis of time-lapse images from the Sugar Bowl camera (Major and others, this volume, chap. 12) and with declining volumetric extrusion rates derived from analysis of digital elevation models (DEMs) for the same period (Schilling and others, this volume, chap. 8).

No additional GPS spiders were deployed to active parts of the growing dome from March to December 2005 because the surface was too steep, too rugged, or too hot. Meanwhile, spiders deployed to older parts of the 2004–5 dome, the 1980–86 dome, and Crater Glacier continued to provide data (LaHusen and others, this volume, chap. 16).

Interferometric Synthetic Aperture Radar (InSAR)

InSAR has been used successfully to study surface deformation at dozens of volcanoes worldwide (for example, Amelung and others, 2000; Zebker and others, 2000; Lu and others, 2007), but at Mount St. Helens three factors have limited its utility. First, EDM and GPS measurements show that any surface displacements that occurred at Mount St. Helens between InSAR's emergence in 1993 (Massonnet and others, 1993) and the start of the 2004–5 eruption were small compared to the resolution of InSAR (2.83 cm/fringe for C-band images; Lisowski and others, this volume, chap. 15). Second, persistent winter snow pack and frequent precipitation destroy coherence, except in small areas above the tree line in summer-to-summer interferograms. Third, the orbital repeat intervals for radar satellites ERS (35 days), RADARSAT (24 days), and ENVISAT (35 days) are too short to capture any slow, preeruption deformation and too long to capture rapid near-vent deformation while an eruption is underway. In the latter case, extreme deformation of the growing dome and displaced glacier make the in-crater part of all interferograms incoherent.

These difficulties with InSAR can be overcome to some extent by "stacking" (averaging) several interferograms for relatively short time periods (so coherence is maintained), which collectively span a period long enough for any deformation signal to emerge from the noise. Stacking works on the premise that a small deformation signal from a fixed source will accumulate with time, while random atmospheric noise sources will tend to cancel. Poland and Lu (this volume, chap. 18) stacked and analyzed hundreds of interferograms of Mount St. Helens acquired by ERS-1/2, ENVISAT, and RADARSAT satellites from 1992 to 2005. Stacks of preeruptive interferograms indicate no sign of volcanowide deformation, which is consistent with trilateration, campaign GPS, and CGPS data for the period from 1992 to 2005 (Lisowski and others, this volume, chap. 15). In contrast, the most reliable stack of coeruptive interferograms shows line-of-sight (LOS) increases (that is, surface subsidence) on the volcano's flanks at rates of 40–50 mm/yr, which is consistent with CGPS results for the coeruptive period.

Time-Lapse Oblique Photography

Several factors contributed to the widespread use of photography, both from aircraft and the ground, to record various aspects of the eruption including (1) growth, deformation, and geomorphic evolution of the lava dome, (2) perturbed motion and deformation of Crater Glacier, and (3) emergence of the lava column from the vent and resulting movement of spines across the crater floor. First, digital cameras are capable of producing high-quality images in near-real time (an advantage over film cameras) that can be shared among colleagues with ease. Second, the perceived level of risk to observers in the crater, especially during early phases of the eruption, was a factor that encouraged remote photo documentation. In hindsight, the 2004–5 eruption has been benign by comparison to most dacite dome eruptions; nonetheless, risks in proximal areas from rockfalls and small explosions were reduced by replacing human observers with cameras, especially for investigations that required repeated observations over long periods of time (for example, time-lapse images of dome growth). Third, it was recognized early in the 2004–5 eruption that cameras were providing a unique and valuable record of the measured pace, longevity, and character of events that transpired in the vent area. An unusual suite of circumstances—gas-poor, crystal-rich magma emerging from an inclined vent on a relatively flat crater floor beneath a newly formed glacier that is contained on three sides by steep crater walls—combined to create an unusual and visually captivating landscape. Over time scales ranging from minutes to months (from drumbeat earthquakes to gouge-covered, laterally mobile, whaleback-shaped spines), the eruption produced a variety of features that are suited to photo documentation and analysis. The following sections summarize two different approaches to time-lapse photo studies of the eruption. More detailed discussions of these and other camera applications can be found in Poland and others (this volume, chap. 11) and Major and others (this volume, chap. 12).

Synoptic Observations of Dome Growth and Glacier Deformation

Mount St. Helens lies 70 km north-northeast of CVO, within sight on a clear day but at a range suitable only for reconnaissance observations. The volcano's 1980 crater opens

to the north, so the view of the current eruption site from CVO is blocked by the volcano's south flank. Continuous surveillance of the eruption by observers within sight of the vent was impractical for logistical reasons, so remote cameras were used instead to track the changing landscape in the crater. Time-lapse photography cannot be construed as deformation monitoring in a classical geodetic sense, but in the 2004–5 eruption, the disruption of the crater floor and glacier was so extreme that cameras became an effective tool for monitoring dramatic changes in the vent area. Elsewhere, CGPS stations and tiltmeters are better suited to measuring strains that are smaller by several orders of magnitude.

The first remote camera station was installed on October 10, 2004, at Sugar Bowl (altitude 1,859 m) on the east side of The Breach (open north end of 1980 crater), 2.3 km north-northeast of the vent. The Sugar Bowl camera recorded the changing morphology of the welt starting one day before emergence of spine 1 on October 11, 2004, followed by development, movement, and disintegration of three prominent whaleback spines (3, 4, and 5). The Sugar Bowl camera was poorly positioned for photographing the disintegration of spine 5 and westward migration of spine 6, which began in early August 2005, because the camera's view was blocked by the 1980–86 dome from August through early October 2005. But by mid-October 2005, spine 7 had grown into the field of view of the Sugar Bowl camera above the profile of the 1980–86 dome, where it remained through the end of 2005. Because the Sugar Bowl camera captured a large part of the dome growth that occurred from mid-October 2004 through December 2005, its images are well suited to systematic quantitative analysis. Major and others (this volume, chap. 12) used the Sugar Bowl images to estimate lineal extrusion rates as a function of time and to infer short-term (days to weeks) variations in the volumetric extrusion rate.

To complement the Sugar Bowl images, two additional camera stations were installed higher on the crater rim in August 2005. Brutus (BRUT) is located at 2,479 m altitude along the northeast rim, 1.1 km east-northeast of the vent. South Rim (SRIM) is located at 2,512 m altitude along the south-southwest crater rim, 0.7 km from the vent. BRUT sees most of the 2004–5 dome and Crater Glacier from the east-northeast; SRIM sees essentially the same area from a reciprocal vantage point.

Camera station Guacamole (GUAC), located at 1,634 m altitude on the floor of The Breach, 2.6 km north of the vent, was added in November 2005. Station GUAC provides a view of the western part of the 2004–5 dome, including spines 6 and 7, and of the deformed east and west arms of Crater Glacier. The lower altitude of GUAC, relative to the other cameras, allows for occasional glimpses under the clouds that obscure views from the higher cameras. See Poland and others (this volume, chap. 11) for additional description of the camera stations and telemetry system, including map locations, equipment used, method of storing and retrieving images, and capability for controlling camera parameters and shooting schedules.

Arguably the greatest value of the remote camera stations lies in the production of time-lapse "movies" (typically one image per day for several days, or all available three-minute images for a 24-hour period) that portray the changing morphology of the dome, deformation of Crater Glacier, rockfall sequences, and patterns of nighttime glow in an intuitive and easy-to-understand format. Several of these sequences are available on the DVD accompanying this volume and on the CVO Web site (http://vulcan.wr.usgs.gov/Volcanoes/MSH/Images/MSH04/repeat_views.html, last accessed January 14, 2008).

High-Resolution, Small Field-of-View Observations of Extrusion Site

In an attempt to capture any short-term (minutes to hours) variations in the lineal extrusion rate and to assess any correlation between these and "drumbeat" earthquakes, we deployed digital cameras with long focal-length lenses and time-lapse controllers at BRUT and on the September 1984 lobe (SEP) of the 1980–86 dome. Drumbeat earthquakes are repetitive, small earthquakes, many with waveforms similar to other drumbeats, that occurred at remarkably constant intervals during the 2004–5 eruption (Moran and others, this volume, chap. 2; Thelen and others, this volume, chap. 4). A correlation between drumbeats and lineal extrusion rate is suggested by a mathematical model that describes the extrusion process in terms of stick-slip motion of a rigid plug under the combined influences of magma pressure, gravity, and friction on the conduit wall (Iverson and others, 2006; Iverson, this volume, chap. 21). To avoid the need for longer-term power and protection from the elements, each of these camera deployments lasted for only a few hours. From BRUT, a Nikon ® CoolPix 990 camera coupled to a 12–36X spotting scope (fig. 4) produces a field of view at the vent (range ~1100 m) of approximately 60×90 m at 12X, or 20×30 m at 36X. From SEP (range ~400 m), the same camera coupled to a Questar ® 700 telephoto lens (3.5-inch diameter, f7.8) fitted with a 24-mm eyepiece (fig. 5) produces a 1.3×1.0 m field of view. Image size of the Nikon ® CoolPix 990 in "fine" resolution mode is 2048×1536 pixels (3.3 megapixels), so using it with the Questar ® 700 from SEP produces an image in which each pixel corresponds to ~0.6 mm on the ground.

Although the Nikon ® CoolPix 990–Questar ® 700 combination deployed at SEP is theoretically capable of millimeter-scale resolution at the vent, two factors combine to degrade the image quality in practice. First is the difficulty in establishing a sufficiently stable base for an imaging system with such high magnification—a problem with two parts. The first, coupling the camera system securely to the ground, can be overcome by mounting the camera and lens to a rigid plate or a short, heavy-duty tripod and by using sandbags to fix the plate or tripod firmly to the ground. The second part of the problem is ground motion associated with incessant drumbeat earthquakes and occasional larger shocks (M_{max} ~3.6).

On five occasions between September 2 and November 18, 2005, we tried frame intervals of 10 s or 30 s for periods of 1–6 hours at times when drumbeats were occurring every 2–3 minutes. Ground shaking is obvious in only a small fraction of the images, as would be expected from the framing interval, shutter speed (0.004–0.5 s), and average time between quakes. Each set of images reveals what appears to be relatively steady motion of the extrusion out of the vent, although any slight displacements of the camera system or underlying ground cannot be distinguished from apparent motion of the extrusion. We tried repeatedly to include in the images some part of the dome or crater wall that was relatively stable, but the camera's limited field of view and depth of field made this difficult and ultimately unproductive.

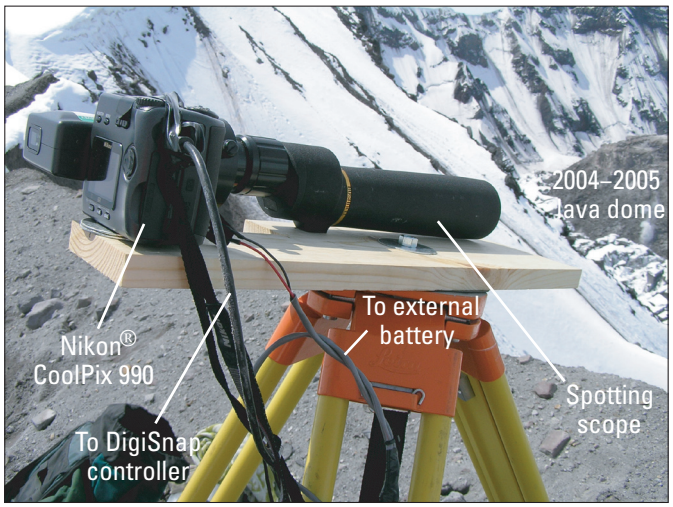

Figure 4. Temporary time-lapse photo station at Brutus (BRUT) on northeast crater rim, Mount St. Helens, Washington. Permanent camera station BRUT is ~100 m north (to the right) of this site.

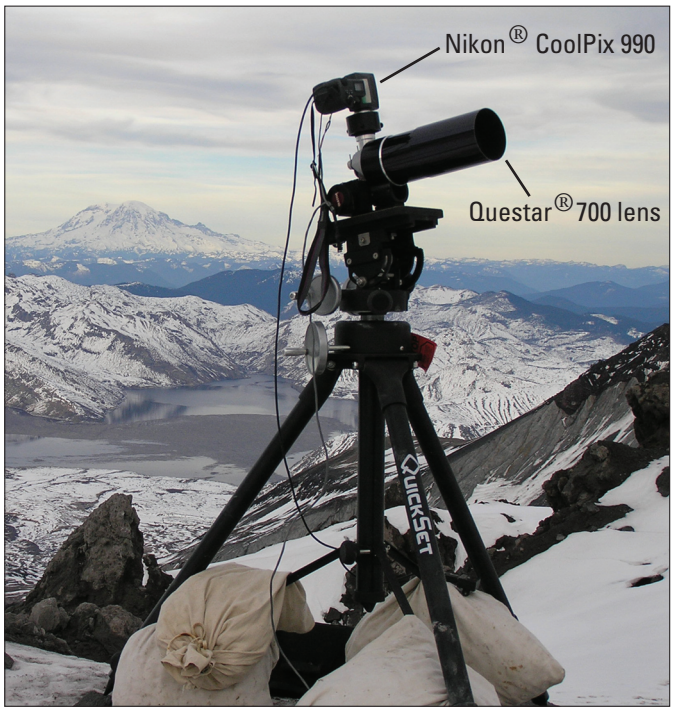

Figure 5. Temporary time-lapse photo station at SEP on September 1984 lobe of 1980–86 dome, ~400 m north of the 2004–5 vent, Mount St. Helens, Washington. Sandbags at base of tripod are for added stability. Spirit Lake near center of photo. Mount Rainier on skyline.

A second factor that contributes to image degradation is heat shimmer caused by uneven refraction of light in unstable air along the camera's line of sight. Heat shimmer is exacerbated by numerous localized heat sources on the 1980–86 and 2004–5 domes and by extensive, hot talus deposits surrounding the active vent. The resulting image degradation can be mitigated to some extent by choosing the line of sight carefully, but this usually comes at the expense of the most desirable framing.

We have been unsuccessful in attempts to capture photographically any jerkiness in the extrusion process that might be associated with drumbeat or larger earthquakes. However, the high-resolution time-lapse images have been useful for another purpose. Because the images are at a known scale (determined empirically by photographing objects of known size with the same camera/lens combination at distances measured using a laser rangefinder), each set of images can be used to measure the average lineal extrusion velocity in the image plane. Motion of the extrusion can be discerned in images acquired only a few minutes apart.

The surface velocity of spine 6 was measured using high-resolution, time-lapse photography from SEP on three occasions from September 2, 2005, to October 18, 2005 (table 1, fig. 6). SEP was due north of the advancing front of spine 6 at the time, so the motion of features through the image frame can be used to measure west and up components of the velocity vector. The resultant velocity (west+up) is a reasonably good indicator of the lineal extrusion rate of spine 6, which was also advancing northward during this period owing to endogenous growth and spreading. The lineal extrusion rate determined in this way declined from 4.51 m/d on September 2 to 4.45 m/d on September 20 and to 2.51 m/d on October 18. Distances from the SEP camera station to the imaged part of spine 6 were measured with a laser rangefinder and are reported as the north component of velocity in table 1. The value for September 2 (>3.3 m/d) is a minimum value because there were no previous rangefinder measurements. The rate was greater than 3.3 m/d, the average value calculated from measurements made on September 2 and September 20, because the extrusion rate and growth rate of spine 6 generally slowed with time.

Figure 6 is based on a subset of 702 images acquired at SEP from 11:14:17 to 17:04:47 PDT (30-s interval) on September 20, 2005. Distance from the camera to the steep, gouge-covered north face of emerging spine 6, measured with a laser rangefinder, was 342±1 m. The camera's field of view included an aluminum target, 46×61 cm in size, for scale. The target was hung by steel cables from an anchor slung by helicopter to the top of the spine. For 58 of the sharpest images, the

pixel coordinates of a distinctive feature on the target relative to a corner of the image were determined by inspection using a PC graphics program. A spreadsheet program was used to convert pixel coordinates to millimeters at the target, using the known image scale, to determine optimal linear fits to the data, to calculate departures from the best-fit line, and to plot the results as a function of time. Average velocity components (that is, slopes of the best-fit lines) are 3.89 m/d west and 2.17 m/d up. Departures from the best-fit lines are irregular and small, on the order of ±10 mm (fig. 6, middle). Therefore, the lineal extrusion rate during a 3.5-hr period on September 20, 2005, was constant within the uncertainty of the measurements. There is no evidence of stick-slip motion of the spine greater than about 10 mm associated with drumbeat earthquakes, which were occurring every 2–3 minutes, nor with two larger shallow quakes at 15:47:19 (M_d 2.9) and 16:05:26 (M_d 1.0) PDT.

Average velocities (west and up) determined from similar observations on September 2, 2005, and October 18, 2005, are 4.51 m/d and 2.51 m/d, respectively (table 1). No comparable measurements were possible from the Sugar Bowl camera on September 2 or September 20, but measurements on October 18, 22, and 24 are in the range 3–4 m/d. In all three cases in which these types of observations were made, the motion of the extruding spine was steady over time scales of a few hours; no evidence of short-term rate variations was seen in any of the photos. However, such variations likely are occurring in the conduit during earthquakes, and variations could also be occurring at the surface in millimeter-scale jerks too small to be resolved by this technique. During the first year of the eruption, drumbeat earthquakes occurred at rates of 0.3–3 per minute, while the lineal extrusion velocity was 1–10 m/d. If all of the motion were associated with drumbeat earthquakes, this would imply an average event size of 2.3 mm/drumbeat at the source. This value for average event size would be smaller if, as seems likely, extrusion is partly aseismic and seismic dislocations are attenuated between the earthquake source area and the surface.

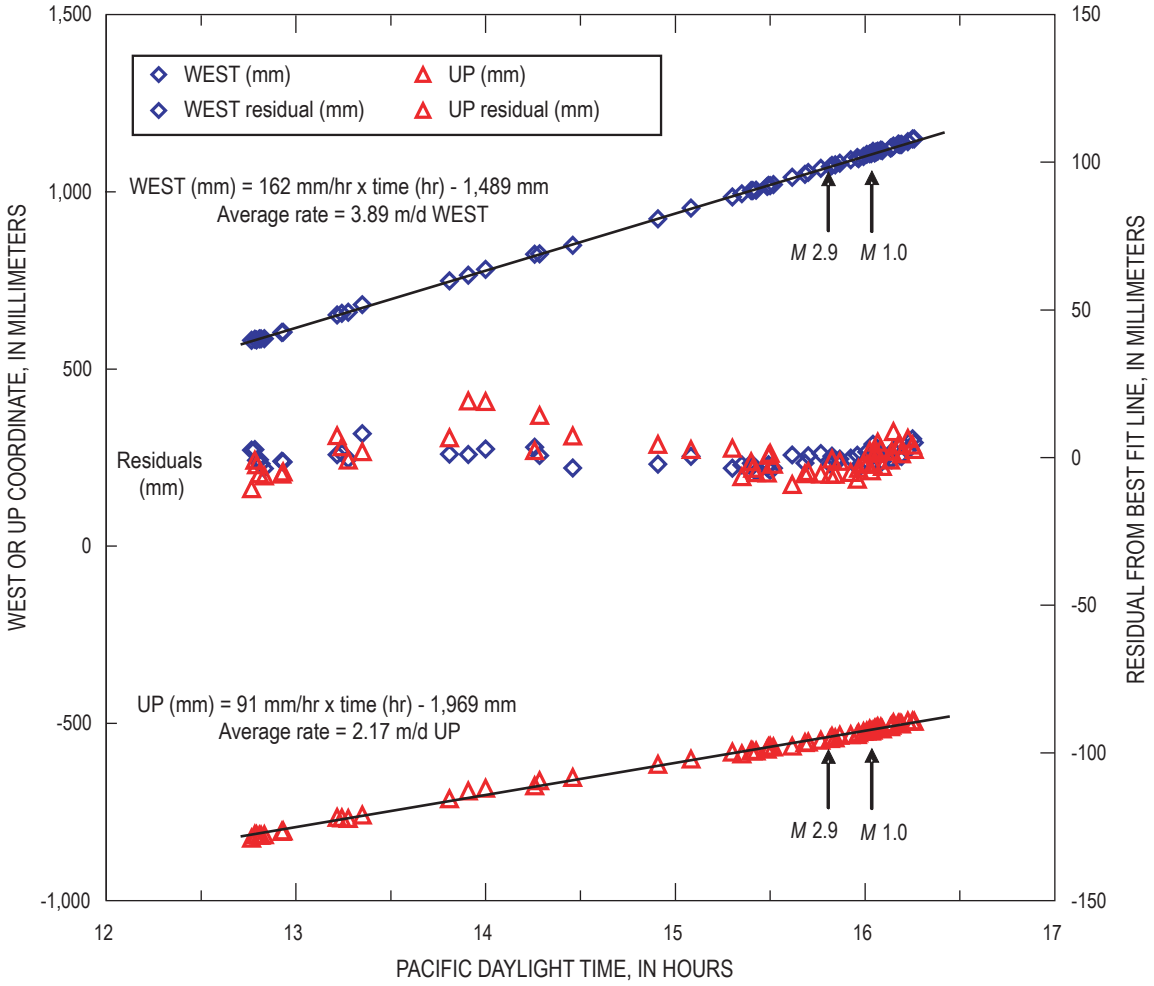

Figure 6. Lineal extrusion velocity of spine 6 for ~3.5-hour period on September 20, 2005, based on analysis of high magnification, small field-of-view, time-lapse (30 s interval) digital images from temporary camera station SEP, Mount St. Helens, Washington. Departures from best-fit lines for west and up components of motion are shown with corresponding symbols in middle ("Residuals").

Table 1. Velocities determined from high-magnification, small field-of-view, time-lapse images at station SEP, Mount St. Helens, Washington.

Date (2005)	West velocity (m/d)	Up velocity (m/d)	Extrusion velocity (west + up) (m/d)	North velocity (m/d)	Distance to target (m)
September 2	4.23	1.55	4.51	>3.3	402
September 20	3.89	2.17	4.45	3.3	342
October 18	2.41	0.69	2.51	1.3	306

Trilateration and Triangulation of Points on the Growing Dome

Classical trilateration and triangulation techniques were adapted with good results to measure changing displacement rates on the growing dome during 1980–86 which, together with changing patterns of seismicity, were used to predict the start of each dome-building episode from a few days to three weeks in advance (Swanson and others, 1983). Measurements were made by affixing prism reflectors to the dome and tracking their motion by using an EDM and theodolite from fixed points on the crater floor or, in some cases, from points on stable parts the dome itself. To increase the number of targets without continuously exposing a large number of reflectors to harsh conditions in the crater, some target points were marked with a survey pin so that a person on foot could accurately position a reflector at the point for a few minutes while a colleague made EDM and theodolite measurements. In this way, more than a dozen survey points distributed across the dome could be surveyed in a few hours.

We tried a similar approach to measure displacement rates on the 2004–5 dome, with lesser success. One difference from the 1980–86 dome is that continuous extrusion, frequent rockfalls, and the deeply crevassed glacier generally precluded foot travel on or around the 2004–5 dome. Instead, five targets, each consisting of a single prism reflector at the center of a painted wooden board attached to a barbell weight as a base, were slung from a helicopter to the 2004–5 dome and Crater Glacier. Three of the targets were set on spine 4, one to the east on rubble of spine 3, and one on the east arm of the glacier. None of the targets could be placed on active spine 5 because it was too steep and hot at the time. All of the targets were observed from BRUT (range ~1,100 m) using a Wild ® TC1000 total station tacheometer on April 21, May 3, and September 20, 2005. The tacheometer can produce surveys with angle measurements accurate to 3 arc seconds at range 1–2.5 km, depending on viewing conditions. Standard deviation of range measurements is 3 mm + 2 ppm, which corresponds to ±5 mm at 1 km range.

Four of the targets survived to the second survey, and three survived to the third survey. However, reflections were obtained from only two targets in the initial survey and from no targets in the second or third surveys, so we lack range measurements for the repeat surveys. The lack of reflections likely resulted from dust clinging to the prisms, etching of the glass by volcanic gases, and (or) changing alignment of the prisms with respect to the sight line as a result of earthquake shaking or slumping. The longest-surviving targets were near the top of spine 4, near the base of spine 3, and on the east arm of the glacier.

For the period May 3 to September 20, 2005, minimum average horizontal velocities of the three surviving targets declined to about one-fourth to one-third of the corresponding values for April 21 to May 3, 2005. For example, the average velocity of a target near the top of spine 4 declined from 0.28 m/d during the early period (April 21 to May 3) to 0.06 m/d during the latter period (May 3 to September 20). For the same periods, the target near the base of spine 3 slowed from 0.09 m/d to 0.02 m/d, and the eastside glacier target slowed from 0.49 m/d to 0.18 m/d. Steep, rugged, and hot terrain on the active dome precluded the use of GPS spiders during this period, so no data are available for comparison. Regardless, the observed slowing trend is consistent with what was happening in the crater at the time. When the first triangulation measurements were made on April 21, 2005, spine 5 was extruding southward, shoving the remnants of spines 3 and 4 southeastward and compressing the east arm of Crater Glacier, which resulted in thickening and increased rate of flow northward (Walder and others, this volume, chap. 13). Spine 6 emerged in early August 2005 and moved westward for the duration of the measurements. The movement of spine 6 eased the stress on spines 3 and 4 and on the glacier's east arm, which caused their velocities to slow.

Total-station surveys made by using helicopter-deployed targets are a feasible, albeit costly and manpower-intensive means to monitor surface displacements on a growing dome. This approach might be cost effective in some situations, but in our case the measurements were abandoned owing to the difficulty of maintaining targets on the dome and the cost of helicopter operations required for each survey. The long sight lines and consequent inability to obtain reflections from the prisms greatly weakened the value of the survey. Although the targets costs less than $200 each, their deployment and initial survey required about one hour of helicopter flight time (~$750/hr), as did each of two repeat surveys spaced 12 days and ~4.5 months apart, resulting in ~1 m accuracy at three

surviving targets. For comparison, a GPS spider costs about $2,500, can be deployed to the dome in about one helicopter flight hour and later retrieved if desired. A spider provides three-dimensional positioning information every few minutes, with an accuracy of a few centimeters, without the need for field personnel, except for deployment and retrieval.

Borehole Tiltmeters

Two Pinnacle 5000 series borehole tiltmeters with tilt resolution of 5×10^{-9} radian (3×10^{-7} angular degree) were installed on the 1980–86 dome to record any transient (seconds to days) ground tilt that might accompany extrusion of the 2004–5 dome and consequent deformation of the crater floor and glacier. The installations were motivated in part by a dynamical model in which stick-slip motion of the plug produces repetitive, reversible strain in host rock near the conduit (Iverson and others, 2006; Iverson, this volume, chap. 21). If each drumbeat earthquake represents an upward "slip" of the plug, followed by a few minutes of increasing magma pressure while the plug remains "stuck," drumbeats should be associated with sudden inward tilt followed by gradual outward tilt between beats.

To test this hypothesis, the first tiltmeter was installed in a 2.3-m-deep hole bored into the September 1984 lobe of the 1980–86 dome (SEP), 480 m N. 16° W. of the 2004–5 vent, on August 5, 2005. A second tiltmeter (REM) was installed in a 1.8-m-deep hole on the northeast sector of the 1980–86 dome, 480 m N. 34° E. of the vent, on November 17, 2004. Both tiltmeters were modified by the manufacturer to enable one-second sampling. Data are telemetered to CVO by way of the U.S. Forest Service's Coldwater Ridge Visitor Center.

Analysis of the tiltmeter records is ongoing, and a complete discussion of results is beyond the scope of this paper. To date, we have seen no evidence of repetitive, reversible tilt events associated with drumbeat earthquakes. It is possible that tilts occur but are too small to be resolved by the tiltmeters, or that the tiltmeters are too far away from the source of the drumbeats. Fractured host rock surrounding the conduit wall or the rubbly interior of the 1980–86 dome might accommodate strains produced by stick-slip motion of the plug without transmitting them to the tiltmeter sites. Without further analysis, this null result should not be interpreted as negative evidence for the occurrence of stick-slip motion as predicted by the model.

Both tiltmeters have recorded tilt changes over time scales of a few minutes to weeks that are likely related to the extrusion process. The azimuths of tilt vectors for many of these events point either toward or away from the extrusion site within a few degrees. Consequently, the vectors from two tiltmeters tend to intersect close to the vent, indicating a shallow pressure source there. It seems plausible that some of the tilt signals are caused by relatively subtle changes in the shallow supply rate or extrusion rate, perhaps related to continual reorganization of the uppermost part of the conduit as the locus of surface activity shifts and the shape of the dome changes. Some of the larger earthquakes (M_d ~2) are associated with tilt events lasting several minutes, but most are not.

A tiltmeter and GPS spider (DOM1), located within 30 m of each other on the September 1984 lobe, responded to some of the same events. For example, the radial tilt component and DOM1 northings increased during September 1–23, 2005, by about 30 microradians and 12 cm, respectively. The instruments are nearly due north of the vent, and both measurements suggest inflation of the vent area. The simplest explanation is that increasing pressure beneath the vent caused the September 1984 lobe to tilt and move northward. At the time, spine 6 was extruding southwestward and migrating westward prior to the emergence of spine 7 in mid-October 2005. Northward tilting and displacement of the September 1984 lobe presaged the emergence of spine 7, possibly during a period of increased extrusion rate. Unfortunately, measurements of the lineal extrusion rate from Sugar Bowl were impossible in September 2005 because the camera's view of spine 6 was blocked by the 1980–86 dome (see earlier section titled Synoptic Observations of Dome Growth and Glacier Deformation).

Discussion

Although some of the techniques discussed above were more successful than others, all of them contributed to our evolving understanding of how Mount St. Helens deformed before and during eruptive activity in 2004–5. Rather than discussing the deformation results separately here, we also consider information from other disciplines (seismology, gas geochemistry, and petrology) and address a few broader issues. Our intent is to characterize current thinking about the eruption and to draw attention to some unresolved questions.

Where, and for how long, was the 2004–5 magma stored before the beginning of unrest on September 23, 2004? What is the nature of the magma reservoir and conduit system? How quickly did the 2004–5 magma rise to the surface? Why was there no inflation at JRO1 prior to September 23, 2004, given that the station clearly responded to deflation and shallow seismicity starting on that date? What are the implications for the future course of this eruption and for anticipating eruptions at similar volcanoes? None of these questions can be answered definitively from the geodetic data alone; however, when combined with other datasets, the geodetic data help to place useful constraints on Mount St. Helens' magma plumbing system and to highlight areas for additional research.

Source Models

The details of various source models fit to the geodetic data are discussed elsewhere in this volume, including Lisowski and others (chap. 15), Poland and Lu (chap. 18), and Mastin and others (chap. 22). Common elements of these source models are (1) depth in the range of 5–12 km (bot-

tom possibly as deep as 20 km), and (2) volume loss through December 2005 in the range 15–30×10^6 m^3, compared to extruded volume of 73×10^6 m^3. Lisowski and others (this volume, chap. 15) modeled and removed the effects of plate motion, regional tectonics, and gravitational loading by the new dome before inverting CGPS data for a best-fit volcanic source model—a point prolate spheroid with its long axis vertical centered near 8 km depth, with a volume loss of 16–24×10^6 m^3 through October 31, 2006. Poland and Lu (this volume, chap. 18) modeled LOS changes from stacked co-eruptive interferograms by using a point source, which best fit the data with a depth of 12 km and a volume loss rate of 27×10^6 m^3/yr. They concluded that a more complicated model is not justified by the InSAR data alone, but they agreed with other authors in the volume that a vertically elongate source is probably more realistic and a better fit to the geodetic dataset as a whole. Mastin and others (this volume, chap. 22) used a vertical ellipsoidal source to fit surface displacements from CGPS data from November 8, 2004, to July 14, 2005. They concluded that the top of the source is 5±1 km deep, but the basal depth is poorly constrained—possibly 10–20 km. Their estimate of source-volume loss during that period is 11–15×10^6 m^3, increasing as the bottom of the source gets deeper. This corresponds to an average volume-loss rate of 16–22×10^6 m^3/yr, which we might double to account for the period of rapid motion at JRO1 from September 23, 2004, to November 8, 2004, which was not included in the model.

These geodetic models generally are consistent with the amount of CO_2 and other volcanic gases emitted during the eruption, which indicate that the erupting magma last equilibrated at 850°C and 130 MPa—conditions corresponding to a reservoir 5.2 km deep (Gerlach and others, this volume, chap. 26). Likewise, samples of the 2004–5 dome indicate that the pressure of last phenocryst growth corresponds to that near the apex of the magma reservoir at a depth of about 5 km (Pallister and others, this volume, chap. 30; Rutherford and Devine, this volume, chap. 31). Pallister and others (this volume, chap. 30) noted the possibility that the 2004–5 magma might be residual from the 1980–86 reservoir and went on to write: "Viewed in the context of seismic, deformation, and gas emission data, the petrologic and geochemical data can be explained by ascent of a geochemically distinct batch of magma into the apex of the [1980–86] reservoir during the period 1987–1997, followed by upward movement of magma into a new conduit, beginning in late September 2004."

In our opinion, the geodetic, gas-emission, and geochemical data from the 2004–5 eruption all point to involvement of magma that was stored in a vertically elongate reservoir centered near 8 km depth and extending upward to about 5 km. We believe this is the same reservoir that fed the plinian eruption of May 18, 1980, smaller explosive eruptions during the summer of 1980, and dome-building eruptions during 1980–86, as inferred by Scandone and Malone (1985) from seismic data (source centered at 9 km, extending from 7 km to 14 km) and Rutherford and others (1985) from the mineral phase assemblage found in May 18 pumice (7.2±1 km). It seems likely that the reservoir was replenished prior to (Moran, 1994; Moran and others, this volume, chap. 2) and possibly during the current eruption (Mastin and others, this volume, chap. 22; Pallister and others, this volume, chap. 30). Data from GPS and InSAR show that most of the surface deformation caused by pre-eruption reservoir inflation occurred prior to 1991, but there is seismic evidence for pressurization of the reservoir and upward fluid intrusion starting in 1987 and continuing at least until 2001. Apparently, reservoir replenishment and surface inflation occurred aseismically until shortly after the extended pause in dome building that began in 1986. Thereafter, increasing strain on rock hosting the reservoir and episodic intrusion of fluids induced microseismicity but no measurable surface deformation.

Implications for the Magma Plumbing System

On September 22, 2004, two things were clear: (1) seismicity at Mount St. Helens was at a low background level characteristic of long periods between sporadic earthquake swarms, and (2) JRO1 was moving northeastward relative to stable North America as part of a tectonic block undergoing clockwise rotation about a pole located either in south-central Oregon (Savage and others, 2000) or along the western part of the Oregon-Washington border where it intersects the Olympic-Wallowa lineament (McCaffrey and others, 2000). The emission rates of volcanic gases probably were low, as they had been each time they were measured after a temporary increase in CO_2 emission was noted during increased seismicity in spring–summer 1998. On four occasions from September 27 to October 2, 2004, measured emission rates of magmatic CO_2 and SO_2 were less than detection thresholds; the first notable increase did not occur until October 3, 2004 (Gerlach and others, this volume, chap. 26).

In hindsight, the September 22 calm belied a volcano poised to erupt. A swarm of small earthquakes, all within 2 km of the crater floor, began around 0200 PDT September 23. By midday on September 28, cracks large enough to be seen from a helicopter flying in the crater appeared in glacier ice on the south crater floor. Rapid uplift and intense seismicity continued for several days, and by October 7, a large welt growing on the south crater floor had approached the height of the 1980–86 dome (fig. 7). The first of several spines emerged from the welt on October 11, less than three weeks after the peaceful dawn of September 22.

Model-derived estimates of source-volume decrease during the first 15 months of the eruption are in the range 15–30×10^6 m^3, compared to an erupted volume of 73±4×10^6 m^3 through December 15, 2005. This suggests, but does not require, that the magma reservoir was partially recharged during the eruption. The lava extrusion rate declined from 5.9 m^3/s to 2.5 m^3/s during the 2.7 months from October 13, 2004, to January 3, 2005, but it varied only between 2.4 m^3/s and 0.7 m^3/s during the ensuing 14 months through the end of 2005 (Schilling and others, this volume, chap. 8). Meanwhile, the

JRO1 displacement rate slowed from a peak value of 0.5 mm/d in late September–early October 2004 to a steady 0.04 mm/d from May through December 2005. These trends suggest that the eruption might be approaching a steady-state condition in which the extrusion rate equals the recharge rate. If so, the situation could persist for years to decades, limited only by the volume of magma available for recharge.

Constraints and Conundrums

The geodetic data help to constrain the depth and geometry of the magma plumbing system and the time history of magma outflow and possible recharge to the reservoir. However, additional questions arise when the geodetic data are considered together with other datasets. For example, why did JRO1 immediately respond to the onset of shallow seismicity, presumably when magma began its ascent, but did not detect any precursory surface deformation during the preceding seven years? The most straightforward answer is that no such deformation occurred because the system was poised to erupt magma stored in the reservoir or conduit system since the 1980–86 eruption, long before JRO1 was installed in May 1997. This idea is consistent with data from trilateration surveys that show surface dilatation, presumably caused by magma accumulation beneath the volcano, between 1982 and 1991. It is also possible that the reservoir inflated during the series of earthquake swarms between 1987 and 2001 by an amount that was too small to cause measurable surface deformation. Mastin and others (this volume, chap. 22) make the point that magma compressibility could have significantly dampened any geodetic signal at Mount St. Helens. Perhaps reservoir magma is compressible enough and the host rock stiff enough that the amount of magma added to the reservoir since 1987 was accommodated without measurably deforming the surface.

How did material that resulted in rapid development of a welt on the south crater floor and subsequent extrusion of highly crystalline, gas-poor magma as gouge-covered spines (Cashman and others, this volume, chap. 19) move through or past the 1980–86 conduit system without substantially deforming more of the volcano and its surroundings? Station JRO1, 9 km north-northwest of the 2004–5 vent, recorded no anoma-

Figure 7. Welt growing on south crater floor, October 7, 2004, as seen from Brutus (BRUT) on northeast crater rim, Mount St. Helens, Washington. South (left) half of the welt is mantled by uplifted glacial ice and ash from small explosions on October 1 and October 5. The north (right) half comprises uplifted crater-floor material and part of the south flank of the 1980–86 dome. The latter was dubbed "Opus area" after 1980s-vintage EDM station Opus, which was located on south side of graben that formed during May 1985 dome-building episode (Swanson and others, 1987).

lous motion at millimeter scale before the eruption. A single-frequency GPS station at SEP on the 1980–86 dome, less than 500 m from the vent, moved anomalously about 20 cm north, 8 cm west, and 12 cm up during the 9-month period ending on September 27, 2004 (LaHusen and others, this volume, chap. 16)—seemingly not enough to accommodate the shallow intrusion of a meters-thick dacite magma body. One possibility is that the conduit is so poorly coupled to the rest of the volcano that the rising magma column was able to push ahead older conduit material, rather than intruding it. Otherwise, the conduit walls and surrounding host rock would have to be implausibly compliant to accommodate an intrusion without causing more widespread deformation.

If the former contents of the conduit were pushed ahead of reservoir magma, when did the latter first reach the surface? If rapid emergence of the first whaleback-shaped extrusion (spine 3) in late October 2004, following the more-labored extrusions of spines 1 and 2, marked the first arrival of reservoir magma, then the volume of conduit material flushed from the system was about 20×10^6 m^3—the volume of surface deformation plus spines on November 4, 2004. The corresponding radius r_c for a cylinder extending from the surface to depth d = 5 km is 35.7 m, or 28.2 m for d = 8 km. Using the volume of material extruded by November 4, 2004 (11.8×10^6 m^3), instead of the volume of surface deformation, we obtain r_c = 27.4 m for d = 5 km, or 21.7 m for d = 8 km. The average ascent rate through the conduit, v_c, assuming reservoir magma began its rise on September 23, 2004, is 120 m/d for d = 5 km, or 190 m/d for d = 8 km. If, instead, reservoir magma arrived at the surface as spine 1 on October 11, 2004, when the volume of the welt was 10.1×10^6 m^3, then r_c = 25.4 m for d = 5 km, or 20.0 m for d = 8 km; and the average ascent rate was 280 m/d (d = 5 km), or 440 m/d (d = 8 km). Thus, for all plausible dimensions of the conduit system, reservoir magma must have reached the surface early in the eruption, probably about the time CO_2 emission rates peaked in October 2004 (Gerlach and others, this volume, chap. 26).

Calculated ascent rates in the conduit exceed observed lineal extrusion rates, v_s = 2–10 m/d, by more than an order of magnitude, so the conduit must widen considerably near the surface. Thornber and others (this volume, chap. 32) reach a similar conclusion (that is, a "wineglass shape" for the conduit) based on their interpretation of amphibole-rim thicknesses in post-November 2004 magma. Equating magma flux through the conduit to that at the surface for d = 8 km, r_c = 28.2 m, v_c = 190 m/d, and v_s = 10 m/d, we obtain a vent radius, r_v, = 125 m and an extrusion rate of 5.7 m^3/s. Using d = 5 km, r_c = 35.7 m, v_c = 120 m/d, and v_s = 10 m/d produces essentially the same results, which are representative of the early part of the eruption. For comparison, Schilling and others (this volume, chap. 8) estimated the vent diameter to be 150–230 m east-west based on partial exposures of the basal perimeters of extruding spines. The north-south vent diameter is unconstrained owing to lack of adequate exposure.

Slowing of the JRO1 displacement rate suggests a corresponding reduction in the net rate at which magma is being withdrawn from the reservoir to a value that might be sustainable for the foreseeable future (0.5–1 m^3/s). If the lesser withdrawal rate is a result of recharge, the eruption could continue indefinitely. On the other hand, in the absence of sufficient recharge, the eruption will end when (1) the reservoir is depleted of eruptible magma, (2) the pressure difference between reservoir and surface falls below some threshold, or (3) friction in the upper part of the conduit chokes off magma flow (that is, stick-slip motion of the plug ceases—the plug stays stuck). In the latter case, increasing magma pressure beneath the plug could eventually result in an explosion; however, the low gas content of the 2004–5 magma makes an explosion less likely than it would be for gas-rich magma.

When gas-saturated magma rises, decreasing lithostatic pressure results in bubble formation. If some of the bubbles rise buoyantly through the magma and escape toward the surface, we might expect an eventual uptick in gas emission rates if, as we suspect, the Mount St. Helens magma reservoir has been recharged during the current eruption. The fact that no such increase was observed through the end of 2005 requires explanation. Emission rates of CO_2, SO_2, and H_2S were negligible during September 27–30, 2004, a period characterized by scrubbing or sealing-in of gases. Several days of wet degassing ensued, when scrubbing by the ground-water system dominated degassing. October 5–6, 2004, marked the beginning of a period of dry degassing when emission rates increased to 800–2,400 metric tons per day (t/d) CO_2, 40–250 t/d SO_2, and 0–10 t/d H_2S (Dzurisin and others, 2005). Throughout 2005, the emission rates of all three gases were near or below the low end of the October 2004 ranges (Gerlach and others, this volume, chap. 26).

It is possible that the 2004–5 eruption was triggered by a recharge event in September 2004 and that gases exsolved from the rising magma made their way to the surface by early October 2004, causing the observed uptick in emission rates; however, this seems unlikely for two reasons. First, the total amount of CO_2 emitted during the eruption is consistent with degassing the volume of magma that reached the surface, assuming the magma last equilibrated at about 5 km depth. In other words, there is no need to invoke recharge to account for the amount of CO_2 emitted. On the contrary, low CO_2 emission rates imply that the reservoir magma is "flat," that is, depleted of any significant exsolved-gas phase that might have accumulated in its upper part (Gerlach and others, this volume, chap. 26). Perhaps the catastrophic landslide and explosive eruptions of 1980 depleted a volatile-rich cap that formed since the end of the Goat Rocks eruptive period in 1857, and any exsolved gases that accumulated since then escaped before the current eruption began.

The second factor that weighs against a recharge event in September 2004 as the cause of increased CO_2 emission in early October is the short time interval involved. If, for example, recharge at 8 km depth beginning on September 23 was responsible for newly-exsolved CO_2 reaching the surface by October 1, the average ascent rate of the gas was ~1 km/d. This ascent rate is far greater than, for example, the

bubble ascent rate of 1.7 m/hr inferred for the 1975 eruption of Mauna Loa volcano, Hawai‘i (Ryan, 1995), even though bubble ascent rates in basalt are likely to be much greater than in dacite. It is possible that the existence of fracture permeability along the margins of the reservoir could allow this constraint to be bypassed. However, it is more straightforward and seems more likely that the source of CO_2 reaching the surface in early October 2004 was the same magma from the conduit or upper part of the reservoir that began extruding shortly thereafter. If so, any volatiles exsolved from magma entering the lower part of the reservoir since the eruption began have not yet fully traversed the length of the reservoir and conduit system. This implies an average rise rate less than about 10 km in 15 months, corresponding to 0.9 m/hr.

The foregoing paragraphs are not meant to imply that a reservoir recharge event could not have occurred during September and October 2004, but rather that such an event, if it did occur, might not have been the source of CO_2 that reached the surface in the next few days. The CO_2 that did reach the surface in early October 2004 could have come from magma previously stored in the conduit or reservoir. Furthermore, the lack of an uptick in CO_2 emission rates since peak values were measured in October 2004 suggests that the path for CO_2 from the base of the reservoir to the surface might be complex and time-consuming to the extent that the CO_2 signature of any recharge that occurred since the 2004–5 eruption began has yet to reach the surface.

Thus, all three of the traditionally reliable eruption precursors (seismicity, ground deformation, and volcanic gas emission) failed to provide warning that an eruption was imminent at Mount St. Helens until a few days before a visible welt appeared at the surface—both in September 2004 and March–April 1980 (the north-flank bulge). Sporadic earthquake swarms beneath the volcano from 1987 to 2003, at least one of which (1998) was accompanied by increased CO_2 emission, provided longer-term but nonspecific forewarning of the current eruption. Data from a single-frequency CGPS station on the 1980–86 dome might have provided several months warning that something anomalous was occurring, but the station was not operational during most of that period, and its data were not analyzed until after the eruption began. Crater-floor deformation might have been hidden beneath thick glacial ice for some time before the first surface cracks were noticed on September 28.

Implications for Volcano Monitoring

One obvious lesson from the 2004–5 eruption is the value of a dense network of CGPS stations operating long before the onset of unrest. The need for CGPS data from proximal stations was addressed at Mount St. Helens only after the 2004–5 eruption began. Most of the ground deformation that accompanied reservoir replenishment following the 1980–86 eruptions had ceased by 1991, before installation of the first CGPS station, JRO1, in 1997. Playing catch-up with a restless volcano is short sighted and dangerous. The best and safest time to install a comprehensive, integrated monitoring system is before unrest begins, when the need for such a system is less apparent.

There is much we do not understand about the 2004–5 eruption of Mount St. Helens, but the challenge does not end there. On January 11, 2006, Augustine Volcano in Cook Inlet, Alaska, began erupting for the first time since 1986. Augustine is a central dome and lava-flow complex surrounded by pyroclastic debris—not unlike Mount St. Helens in several respects. Both volcanoes are relatively young and frequently active. Mount St. Helens is notorious for its debris avalanche and eruption of May 18, 1980; Augustine has produced at least 11 debris avalanches in the past 2,000 years as a result of summit dome collapses (Waitt and Beget, 1996; Beget and Kienle, 1992). Mount St. Helens' eruptive products range from basalt through dacite (dominantly dacite). Augustine's products are dominantly andesite with small amounts of basaltic andesite and dacite. Before their current eruptions, both volcanoes last erupted in 1986, and both eruptions were dome-building events (Mount St. Helens, 1980–86; Augustine, March–September, 1986).

Given these similarities, we might expect that the precursors to Mount St. Helens' and Augustine's most recent eruptions were similar, too, and in several respects they were; however, there were some striking differences. On November 29, 2005, the Alaska Volcano Observatory (AVO) released the following statement (http://www.avo.alaska.edu/activity/avoreport.php?view=info&id=342&type=info&month=November&year=2005, last accessed January 14, 2008):

> Beginning in May 2005, there has been a slow increase in the number of earthquakes located under Augustine Volcano. The earthquakes are generally small (less than magnitude 1.0) and concentrate roughly 1 km below the volcano's summit. These earthquakes have slowly increased from 4–8 earthquakes/day to 20–35 earthquakes/day. Additionally, data from a 6-station Global Positioning System (GPS) network on Augustine Volcano indicate that a slow, steady inflation of the volcano started in mid-summer 2005 and continues at present. The GPS benchmark located nearest the summit has moved a total of 2.5 cm (1 inch). This motion is consistent with a source of inflation or pressure change centered under the volcano. This is the first such deformation detected at Augustine Volcano since measurements began just prior to the 1986 eruption.

Small explosions began on December 9, 2005, and there were reports of unusual "steaming" and sulfur smell downwind of the volcano, as well as a visible, condensed-steam plume extending at least 75 km from the volcano on December 12. The eruption began in earnest on January 11, 2006, characterized by magmatic explosions, pyroclastic flows and lahars, and extrusion of a new lava dome and flow that was first observed on January 16, 2006. Emission rates for SO_2 were about 1,000 t/d in early January and several thousand t/d during the first week of the eruption. Corresponding CO_2 emission rates were 2–3 times greater (Cervelli and others, 2006; Power and others, 2006).

The Augustine and Mount St. Helens eruptions were similar in the following respects:

1. No precursory inflation of a deep (>5 km) source was detected; modeling of GPS data indicates the preeruptive inflation source at Augustine was 1–2 km beneath the volcano's summit, at a depth of approximately sea level (Cervelli and others, 2006),

2. Deep deflation was associated with extrusion,

3. Phreatic explosions preceded the beginning of extrusion,

4. Energetic swarms of shallow earthquakes occurred in the days prior to the first explosion, and

5. Erupted products were predominantly effusive, with only minor tephra.

The eruptions differed in the following ways:

6. There were eight months of elevated seismicity at Augustine versus a few days of elevated seismicity at Mount St. Helens,

7. There were six months of precursory inflation at Augustine versus no precursory inflation at Mount St. Helens (but see below), and

8. There were several thousand tons per day of SO_2 and CO_2 recorded at Augustine versus 40–250 t/d SO_2 and 800–2,400 t/d CO_2 recorded at Mount St. Helens (Gerlach and others, this volume, chap. 26).

The differences in items 6 and 8 are supported by unambiguous seismic and gas emission-rate data, but the apparent lack of precursory inflation at Mount St. Helens (item 7) could be an artifact of inadequate geodetic monitoring. Station JRO1 might have been too distant (9 km) to detect inflation of a shallow source comparable to the one that inflated for months at Augustine. Even so, relatively deep sources at both volcanoes deflated during the eruptions but did not inflate in the years or months beforehand—a pattern unlikely to be sustainable over several eruption cycles. A possible explanation for this observation is that inflation of deep magma sources beneath arc volcanoes occurs mainly early in the eruption cycle, soon after an eruption ends, and slows as the next eruption approaches. This pattern has been observed in InSAR studies of Westdahl and Okmok volcanoes in the Aleutian arc by Lu and others (2003, 2005). Lu and his colleagues suggest that the magma supply rate is governed by the pressure gradient between a deep source and shallow reservoir. The pressure gradient and hence the flow rate are greatest immediately after eruptions. Pressurization of the reservoir decreases both the pressure gradient and flow rate, but eventually the reservoir ruptures, an eruption or intrusion occurs, and the cycle starts anew. This scenario is consistent with trilateration and campaign GPS results for Mount St. Helens that showed dilatation between 1982 and 1991, but no measurable deformation from 1991 to 2000 or from 2000 to 2003.

Given that the latest repose periods at Mount St. Helens and Augustine were similar, and that the magma erupted at Mount St. Helens is more viscous (greater SiO_2 content and crystallinity, lower temperature), why did Mount St. Helens erupt with less precursory seismicity and (perhaps) surface deformation? An important difference between the two eruptions is the higher gas-emission rates at Augustine. Gassy magma suggests a deep source, and the prolonged period of elevated seismicity and surface inflation at Augustine probably reflect the accumulation of rising magma in a shallow reservoir. In contrast, there are indications that gas-poor 2004–5 magma had already accumulated in a crustal reservoir long before the September 2004 earthquake swarm at Mount St. Helens. Inflation might have occurred anytime between 1982 and 1991, as suggested by trilateration and GPS results, episodically during repeated earthquake swarms between 1987 and 2001, or continuously and mostly aseismically.

Conjecture Regarding the Link Between 1980–1986 and 2004–2005 Eruptions

Continued low gas-emission rates at Mount St. Helens more than a year after the eruption began, and after extrusion of more than 73×10^6 m^3 of dacite, suggest that the eruption is being fed from a reservoir of mostly degassed magma. The most likely source is magma left over from the 1980s. The May 18, 1980, eruption was unusual in that it was triggered by a large landslide at 0832 PDT that unloaded the magmatic system suddenly and tapped gas-rich magma from a reservoir at 8 km depth. A devastating lateral blast and debris avalanche produced the most compelling images from the eruption, but an important change in the eruption's character did not occur until midday. Rowley and others (1981, p. 492, 489) reported: "At about noon, the eruption cloud lightened in color from medium gray to dirty white * * * (D.A. Swanson, oral commun., 1980)." and "Pyroclastic flows were first observed being emplaced at 1217 PDT (Pacific Daylight time) on May 18, nearly 4 hr after the start of the eruption, and successive pyroclastic flows continued to form intermittently for about 5 hr thereafter." It seems likely that the change in the eruption cloud at midday corresponded to the first arrival at the surface of gas-rich magma from a deeper source, presumably the 7-km-deep reservoir proposed by Rutherford and others (1985). This idea is consistent with the onset of vigorous harmonic tremor, indicative of magma movement, just before noon, and with its decline at about 1730 PDT (Malone and others, 1981).

If this scenario is correct, the hours-long delay between the initiation of the landslide and the first arrival of reservoir magma at the surface suggests that the latter might not have occurred without the former, that is, that the landslide interrupted a sequence of events that otherwise might not have tapped the reservoir on May 18. Without the landslide trigger, magma intruding the volcano to cause the famous north-flank bulge might have reached the surface in less spectacular fash-

ion and might not have been followed by gas-rich magma from the reservoir. We speculate that catastrophic unloading of the magmatic system by the landslide decreased the reservoir-to-surface distance, thus increasing the pressure gradient abruptly. As a consequence of the greater pressure gradient, rapidly rising magma created and maintained an open conduit to the surface for 9 hours—enough time to release any separate gas phase that might have accumulated near the top of the reservoir. There would have been ample time, since the end of the previous eruption in 1857, for a volatile-rich cap to form by vesiculation and bubble-rise in the reservoir. Magma that rose into the lower-pressure environment of the reservoir prior to 1980 would have been temporarily oversaturated in volatiles. The "excess" volatiles would have exsolved to form bubbles that tend to aggregate and migrate toward the top of the reservoir. Given enough time and low enough permeability to the surface, a volatile-rich cap develops on the reservoir. The physics of this process is beyond the scope of this paper. We suggest only that the May 18, 1980, landslide might have initiated a cascade of events that resulted in, among the more obvious consequences, catastrophic loss of the gas-rich upper part of the reservoir. This set the stage for dome-building eruptions that followed in 1980–86 and 2004–5, which tapped reservoir magma that had been separated from its excess volatiles and only partly replenished during the interim.

The presence in the upper crust of magma remnant from the 1980s and earlier, which was devoid of its excess volatiles as a result of the May 18, 1980, eruption, might explain some aspects of the 2004–5 eruption. For example, the absence of precursory reservoir inflation is consistent with the idea that the magma erupted in 2004–5 was already present in the reservoir and conduit system when JRO1 was installed in 1997. Likewise, the short duration of precursory seismicity and the low gas emission rates throughout the 2004–5 eruption can be explained if the first few days of unrest involved the mobilization of magma that had been stored in the upper part of the conduit since the end of the 1980–86 eruption. This was soon followed by the rise of magma that arrived in the reservoir sometime before 1980, equilibrated to the pressure and temperature conditions in the reservoir, and lost its excess volatiles during the eruption on May 18, 1980. This explanation does not preclude partial recharge of the reservoir prior to or during the 2004–5 eruption. Mastin and others (this volume, chap. 22) conclude from their analysis of the geodetic data that " * * * erupted magma has been replaced in increasing proportions by recharge, but that the recharge rate remains somewhat less than the current effusion rate." Both the velocity of JRO1 and the effusion rate declined throughout 2006–7. During part or all of that period, the recharge rate might have been comparable to the effusion rate (L. Mastin, oral commun., 2008).

Although mostly speculative, we believe the following scenario is consistent with the current state of knowledge concerning the 1980–86 and 2004–5 eruptions. Both eruptions were fed from a reservoir centered near 8 km depth; magma erupted in the 1980s accumulated in the reservoir during an extended period, long enough for gas bubbles to rise and form a volatile-rich cap (Gerlach and McGee, 1994). The May 18, 1980, landslide and plinian eruption depressurized the reservoir catastrophically, releasing the volatile-rich cap and causing additional bubbles to form throughout the reservoir. Most of those bubbles managed to rise to the top of the reservoir at about 5 km depth and escape via the 1980 conduit system prior to the start of the 2004–5 eruption, leaving behind a large volume of gas-poor magma—at least several cubic kilometers according to Mastin and others (this volume, chap. 22). The 2004–5 eruption was preceded by and has been accompanied by reservoir recharge, which is continuing at a rate of ~1 m^3/s (early 2006). Any magmatic gas signature from recharge might be delayed and muted by the large vertical extent of the reservoir and relatively high viscosity of reservoir magma. Factors that will influence the future course of the eruption (for example, slowing and eventual cessation of dome growth, or a transition to either more explosive activity or effusion of more mafic magma) include (1) the recharge rate going forward, (2) bubble-rise rates in the reservoir–conduit system, and (3) the character of magma entering the base of the reservoir (that is, gas content and melt composition).

Volcanoes are complex natural systems. Effective hazards mitigation, even at well-monitored volcanoes such as Mount St. Helens, requires constant vigilance and better understanding of a wide variety of physical, chemical, and hydrologic processes that interact to produce eruptions. The events of late 2004 and 2005 at Mount St. Helens amazed and confounded us as they unfolded, and to some extent they still do. What were the perceived odds on September 22, 2004, that an enormous welt would rise on the crater floor in a matter of days, without producing far-field deformation, deep seismicity, or greatly increased gas emission? Or that the top of a dacite magma column would emerge from the welt in less than three weeks and extrude for more than a year as a series of gouge-covered spines, with older spines shunted aside as newer ones emerged? Or that during the eruption, Crater Glacier would be split in two and crumpled against the crater walls without producing even a trickle of water flow at the crater mouth? Clearly, there is much left to learn at this volcano before we can understand how, when, and why such amazing events occur, and to what extent they might be hazardous.

Acknowledgments

This is an overview and ideas paper, mostly devoid of its own data. The authors make no claim of originality or exclusivity. We accept responsibility for bad or half-baked ideas and credit any good ones to the eruption team at the USGS Cascades Volcano Observatory. We thank L.G. Mastin and P.F. Cervelli for helpful reviews.

References Cited

Amelung, F., Jónsson, S., Zebker, H., and Segall, P., 2000, Widespread uplift and 'trapdoor' faulting on Galápagos volcanoes observed with radar interferometry: Nature, v. 407, no. 6807, p. 993–996.

Beget, J.E., and Kienle, J., 1992, Cyclic formation of debris avalanches at Mount St. Augustine volcano: Nature, v. 356, no. 6371, p. 701–704.

Caputo, M., 1979, Two thousand years of geodetic and geophysical observations in the Phlegraean Fields near Naples: Geophysical Journal of the Royal Astronomical Society, v. 56, p. 319–328.

Cashman, K.V., Thornber, C.R., and Pallister, J.S., 2008, From dome to dust; shallow crystallization and fragmentation of conduit magma during the 2004–2006 dome extrusion of Mount St. Helens, Washington, chap. 19 *of* Sherrod, D.R., Scott, W.E., and Stauffer, P.H., eds., A volcano rekindled; the renewed eruption of Mount St. Helens, 2004–2006: U.S. Geological Survey Professional Paper 1750 (this volume).

Cervelli, P.F., Fournier, T., Freymueller, J., and Power, J.A., 2006, Ground deformation associated with the precursory unrest and early phases of the January 2006 eruption of Augustine Volcano, Alaska: Geophysical Research Letters, v. 33, L18304, doi: 10.1029/2006GL027219.

Dvorak, J.J., and Okamura, A.T., 1987, A hydraulic model to explain variations in summit tilt rate at Kilauea and Mauna Loa volcanoes, chap. 46 *of* Decker, R.W., Wright, T.L., and Stauffer, P.H., eds., Volcanism in Hawaii: U.S. Geological Survey Professional Paper 1350, v. 2, p. 1281–1296.

Dzurisin, D., 2003, A comprehensive approach to monitoring volcano deformation as a window on the eruption cycle: Reviews of Geophysics, v. 41, no. 1, p. 1.1–1.29, doi:10.1029/2001RG000107.

Dzurisin, D., Wicks, C., Jr., and Thatcher, W., 1999, Renewed uplift at the Yellowstone caldera measured by leveling surveys and satellite radar interferometry: Bulletin of Volcanology, v. 61, p. 349–355.

Dzurisin, D., Vallance, J.W., Gerlach, T.M., Moran, S.C., and Malone, S.D., 2005, Mount St. Helens reawakens: Eos (American Geophysical Union Transactions), v. 86, no. 3, p. 25, 29.

Gerlach, T.M., McGee, K.A., and Doukas, M.P., 2008, Emission rates of CO_2, SO_2, and H_2S, scrubbing, and preeruption excess volatiles at Mount St. Helens, 2004–2005, chap. 26 *of* Sherrod, D.R., Scott, W.E., and Stauffer, P.H., eds., A volcano rekindled; the renewed eruption of Mount St. Helens, 2004–2006: U.S. Geological Survey Professional Paper 1750 (this volume).

Herd, R.A., Edmonds, M., and Bass, V.A., 2005, Catastrophic lava dome failure at Soufrière Hills Volcano, Montserrat, 12–13 July 2003: Journal of Volcanology and Geothermal Research, v. 148, nos. 3–4, p. 234–252, doi:10.1016/j.jvolgeores.2005.05.003.

Hill, D.P., Bailey, R.A., and Ryall, A.S., 1985, Active tectonic and magmatic processes beneath Long Valley caldera, eastern California; an overview: Journal of Geophysical Research, v. 90, p. 11111–11120.

Iverson, R.M., 2008, Dynamics of seismogenic volcanic extrusion resisted by a solid surface plug, Mount St. Helens, 2004–2005, chap. 21 *of* Sherrod, D.R., Scott, W.E., and Stauffer, P.H., eds., A volcano rekindled; the renewed eruption of Mount St. Helens, 2004–2006: U.S. Geological Survey Professional Paper 1750 (this volume).

Iverson, R.M., Dzurisin, Daniel, Gardner, C.A., Gerlach, T.M., LaHusen, R.G., Lisowski, Michael, Major, J.J., Malone, S.D., Messerich, J.A., Moran, S.C., Pallister, J.S., Qamar, A.I., Schilling, S.P., and Vallance, J.W., 2006, Dynamics of seismogenic volcanic extrusion at Mount St. Helens in 2004–05: Nature, v. 444, no. 7118, p. 439–443, doi:10.1038/nature05322.

LaHusen, R.G., Swinford, K.J., Logan, M., and Lisowski, M., 2008, Instrumentation in remote and dangerous settings; examples using data from GPS "spider" deployments during the 2004–2005 eruption of Mount St. Helens, Washington, chap. 16 *of* Sherrod, D.R., Scott, W.E., and Stauffer, P.H., eds., A volcano rekindled; the renewed eruption of Mount St. Helens, 2004–2006: U.S. Geological Survey Professional Paper 1750 (this volume).

Lipman, P.W., Moore, J.G., and Swanson, D.A., 1981, Bulging of the north flank before the May 18 eruption—geodetic data, *in* Lipman, P.W., and Mullineaux, D.R., eds., The 1980 eruptions of Mount St. Helens, Washington: U.S. Geological Survey Professional Paper 1250, p. 143–155.

Lisowski, M., Dzurisin, D., Denlinger, R.P., and Iwatsubo, E.Y., 2008, Analysis of GPS-measured deformation associated with the 2004–2006 dome-building eruption of Mount St. Helens, Washington, chap. 15 *of* Sherrod, D.R., Scott, W.E., and Stauffer, P.H., eds., A volcano rekindled; the renewed eruption of Mount St. Helens, 2004–2006: U.S. Geological Survey Professional Paper 1750 (this volume).

Lu, Z., Masterlark, T., Dzurisin, D., Rykhus, R., and Wicks, C., Jr., 2003, Magma supply dynamics at Westdahl volcano, Alaska, modeled from satellite radar interferometry: Journal of Geophysical Research, v. 108, no. B7, 2354, 17 p., doi:10.1029/2002JB002311.

Lu, Z., Masterlark, T., and Dzurisin, D., 2005, Interferometric synthetic aperture radar (InSAR) Study of Okmok Volcano, Alaska, 1992–2003; magma supply dynamics and post-emplacement lava flow deformation: Journal

of Geophysical Research, v. 110, no. B12, B02403, doi: 10.1029/2004JB003148, 18 p.

Lu, Z., Dzurisin, D., Wicks, C., Jr., Power, J., Kwoun, O., and Rykhus, R., 2007, Diverse deformation patterns of Aleutian volcanoes from satellite interferometric synthetic aperture radar (InSAR), *in* Eichelberger, J.C., Gordeev, E., Izbekov, P., Kasahara, M., and Lees, J.M., eds., Volcanism and tectonics of the Kamchatka Peninsula and adjacent arcs: American Geophysical Union Geophysical Monograph 172, p. 249–261.

Major, J.J., Kingsbury, C.G., Poland, M.P., and LaHusen, R.G., 2008, Extrusion rate of the Mount St. Helens lava dome estimated from terrestrial imagery, November 2004–December 2005, chap. 12 *of* Sherrod, D.R., Scott, W.E., and Stauffer, P.H., eds., A volcano rekindled; the renewed eruption of Mount St. Helens, 2004–2006: U.S. Geological Survey Professional Paper 1750 (this volume).

Malone, S.D., Endo, E.T., Weaver, C.S., and Ramey, J.W., 1981, Seismic monitoring for eruption prediction, *in* Lipman, P.W., and Mullineaux, D.R., eds., The 1980 eruptions of Mount St. Helens, Washington: U.S. Geological Survey Professional Paper 1250, p. 803–813.

Mastin, L.G., Roeloffs, E., Beeler, N.M., and Quick, J.E., 2008, Constraints on the size, overpressure, and volatile content of the Mount St. Helens magma system from geodetic and dome-growth measurements during the 2004–2006+ eruption, chap. 22 *of* Sherrod, D.R., Scott, W.E., and Stauffer, P.H., eds., A volcano rekindled; the renewed eruption of Mount St. Helens, 2004–2006: U.S. Geological Survey Professional Paper 1750 (this volume).

Massonnet, D., Rossi, M., Carmona, C., Adragna, F., Peltzer, G., Feigl, K., and Rabaute, T., 1993, The displacement field of the Landers earthquake mapped by radar interferometry: Nature, v. 364, p. 138–142.

McCaffrey, R., Long, M.D., Goldfinger, C., Zwick, P.C., Nabelek, J.L., Johnson, C.K., and Smith, C., 2000, Rotation and plate locking at the southern Cascadia subduction zone: Geophysical Research Letters, v. 27, no. 19, p. 3117–3120.

Moran, S.C., 1994, Seismicity at Mount St. Helens, 1987–1992: Evidence for repressurization of an active magmatic system: Journal of Geophysical Research, v. 99, p. 4341–4354.

Moran, S.C., Malone, S.D., Qamar, A.I., Thelen, W.A., Wright, A.K., and Caplan-Auerbach, J., 2008, Seismicity associated with renewed dome building at Mount St. Helens, 2004–2005, chap. 2 *of* Sherrod, D.R., Scott, W.E., and Stauffer, P.H., eds., A volcano rekindled; the renewed eruption of Mount St. Helens, 2004–2006: U.S. Geological Survey Professional Paper 1750 (this volume).

Pallister, J.S., Thornber, C.R., Cashman, K.V., Clynne, M.A., Lowers, H.A., Mandeville, C.W., Brownfield, I.K., and Meeker, G.P., 2008, Petrology of the 2004–2006 Mount St. Helens lava dome—implications for magmatic plumbing and eruption triggering, chap. 30 *of* Sherrod, D.R., Scott, W.E., and Stauffer, P.H., eds., A volcano rekindled; the renewed eruption of Mount St. Helens, 2004–2006: U.S. Geological Survey Professional Paper 1750 (this volume).

Poland, M.P., and Lu, Z., 2008, Radar interferometry observations of surface displacements during pre- and coeruptive periods at Mount St. Helens, Washington, 1992–2005, chap. 18 *of* Sherrod, D.R., Scott, W.E., and Stauffer, P.H., eds., A volcano rekindled; the renewed eruption of Mount St. Helens, 2004–2006: U.S. Geological Survey Professional Paper 1750 (this volume).

Poland, M.P., Dzurisin, D., LaHusen, R.G., Major, J.J., Lapcewich, D., Endo, E.T., Gooding, D.J., Schilling, S.P., and Janda, C.G., 2008, Remote camera observations of lava dome growth at Mount St. Helens, Washington, October 2004 to February 2006, chap. 11 *of* Sherrod, D.R., Scott, W.E., and Stauffer, P.H., eds., A volcano rekindled; the renewed eruption of Mount St. Helens, 2004–2006: U.S. Geological Survey Professional Paper 1750 (this volume).

Power, J.A., Nye, C.J., Coombs, M.L., Wessels, R.L., Cervelli, P.F., Dehn, J., Wallace, K.L., Freymueller, J.T., and Doukas, M.P., 2006, The reawakening of Alaska's Augustine Volcano [abs.]: Eos (American Geophysical Union Transactions), v. 87, no. 37, p. 373, doi:10.1029/2006EO370002.

Rowley, P.D., Kuntz, M.A., and MacLeod, N.S., 1981, Pyroclastic-flow deposits, *in* Lipman, P.W., and Mullineaux, D.R., eds., The 1980 eruptions of Mount St. Helens, Washington: U.S. Geological Survey Professional Paper 1250, p. 489–512.

Rutherford, M.J., and Devine, J.D., III, 2008, Magmatic conditions and processes in the storage zone of the 2004–2006 Mount St. Helens dacite, chap. 31 *of* Sherrod, D.R., Scott, W.E., and Stauffer, P.H., eds., A volcano rekindled; the renewed eruption of Mount St. Helens, 2004–2006: U.S. Geological Survey Professional Paper 1750 (this volume).

Rutherford, M.J., Sigurdsson, H., Carey, S., and Davis, A., 1985, The May 18, 1980, eruption of Mount St. Helens; 1. melt composition and experimental phase equilibria: Journal of Geophysical Research, v. 90, no. B4, p. 2929–2947.

Ryan, S.C., 1995, Quiescent outgassing of Mauna Loa volcano, 1958–1994, *in* Rhodes, J.M., and Lockwood, J.P., eds., Mauna Loa revealed; structure, composition, history, and hazards: Washington, D.C., American Geophysical Union Geophysical Monograph 92, p. 95–116.

Savage, J.C., Svarc, J.L., Prescott, W.H., and Murray, M.H., 2000, Deformation across the forearc of the Cascadia subduction zone at Cape Blanco, Oregon: Journal of Geophysical Research, v. 105, no. B2, p. 3095–3102.

Scandone, R., and Malone, S.D., 1985, Magma supply, magma discharge and readjustment of the feeding system of Mount St. Helens during 1980: Journal of Volcanology and Geothermal Research, v. 23, nos. 3–4, p. 239–262, doi:10.1016/0377-0273(85)90036-8.

Schilling, S.P., Thompson, R.A., Messerich, J.A., and Iwatsubo, E.Y., 2008, Use of digital aerophotogrammetry to determine rates of lava dome growth, Mount St. Helens, Washington, 2004–2005, chap. 8 *of* Sherrod, D.R., Scott, W.E., and Stauffer, P.H., eds., A volcano rekindled; the renewed eruption of Mount St. Helens, 2004–2006: U.S. Geological Survey Professional Paper 1750 (this volume).

Swanson, D.A., Lipman, P.W., Moore, J.G., Heliker, C.C., and Yamashita, K.M., 1981, Geodetic monitoring after the May 18 eruption, *in* Lipman, P.W., and Mullineaux, D.R., eds., The 1980 eruptions of Mount St. Helens, Washington: U.S. Geological Survey Professional Paper 1250, p. 157–168.

Swanson, D.A., Casadevall, T.J., Dzurisin, D., Malone, S.D., Newhall, C.G., and Weaver, C.S., 1983, Predicting eruptions at Mount St. Helens, June 1980 through December 1982: Science, v. 221, no. 4618, p. 1369–1376.

Swanson, D.A., Dzurisin, D., Holcomb, R.T., Iwatsubo, E.Y., Chadwick, W.W., Jr., Casadevall, T.J., Ewert, J.W., and Heliker, C.C., 1987, Growth of the lava dome at Mount St. Helens, Washington (USA), 1981–1983*, in* Fink, J.H., ed., Emplacement of silicic domes and lava flows: Geological Society of America Special Paper 212, p. 1–16.

Thelen, W.A., Crosson, R.S., and Creager, K.C., 2008, Absolute and relative locations of earthquakes at Mount St. Helens, Washington, using continuous data; implications for magmatic processes, chap. 4 *of* Sherrod, D.R., Scott, W.E., and Stauffer, P.H., eds., A volcano rekindled; the renewed eruption of Mount St. Helens, 2004–2006: U.S. Geological Survey Professional Paper 1750 (this volume).

Tryggvason, E., 1994, Surface deformation at the Krafla volcano, North Iceland, 1982–1992: Bulletin of Volcanology, v. 56, no. 2, p. 98–107.

Vallance, J.W., Schneider, D.J., and Schilling, S.P., 2008, Growth of the 2004–2006 lava-dome complex at Mount St. Helens, Washington, chap. 9 *of* Sherrod, D.R., Scott, W.E., and Stauffer, P.H., eds., A volcano rekindled; the renewed eruption of Mount St. Helens, 2004–2006: U.S. Geological Survey Professional Paper 1750 (this volume).

Waitt, R.B., and Beget, J.E., 1996, Provisional geologic map of Augustine Volcano, Alaska: U.S. Geological Survey Open-File Report 96–0516, 44 p., 1 plate, scale 1:25,000.

Walder, J.S., Schilling, S.P., Vallance, J.W., and LaHusen, R.G., 2008, Effects of lava-dome growth on the Crater Glacier of Mount St. Helens, Washington, chap. 13 *of* Sherrod, D.R., Scott, W.E., and Stauffer, P.H., eds., A volcano rekindled; the renewed eruption of Mount St. Helens, 2004–2006: U.S. Geological Survey Professional Paper 1750 (this volume).

Wicks, C.W., Thatcher, W., Dzurisin, D., and Svarc, J., 2006, Uplift, thermal unrest, and magma intrusion at Yellowstone caldera: Nature, v. 440, no. 7080, p. 72–75, doi:10.1038/nature04507.

Zebker, H.A., Amelung, F., and Jonsson, S., 2000, Remote sensing of volcano surface and internal processes using radar interferometry, *in* Mouginis-Mark, P.J., Crisp, J.A., and Fink, J.H., eds., Remote sensing of active volcanism: American Geophysical Union Geophysical Monograph 116, p. 179–205.